Int. J. Exp. Path. (2009), 90, 558–574
doi: 10.1111/j.1365-2613.2009.00667.x

ORIGINAL ARTICLE

Mutated K-*ras*^{Asp12} promotes tumourigenesis in *Apc*^{Min} mice more in the large than the small intestines, with synergistic effects between K-*ras* and *Wnt* pathways

Feijun Luo*, David G. Brooks*, Hongtao Ye*, Rifat Hamoudi*, George Poulogiannis*, Charles E. Patek†, Douglas J. Winton‡ and Mark J. Arends*

*Department of Pathology, Addenbrooke's Hospital, University of Cambridge, Cambridge, UK, †Sir Alastair Currie Cancer Research UK Laboratories, Molecular Medicine Centre, Western General Hospital, University of Edinburgh, Edinburgh, UK and ‡Department of Oncology, CRUK Cambridge Research Institute, Addenbrooke's Hospital Campus, University of Cambridge, Cambridge, UK

INTERNATIONAL JOURNAL OF EXPERIMENTAL PATHOLOGY

Summary

K-*ras* mutations are found in 40–50% of human colorectal adenomas and carcinomas, but their functional contribution remains incompletely understood. Here, we show that a conditional mutant K-*ras* mouse model (K-*ras*^{Asp12}/*Cre*), with transient intestinal *Cre* activation by β-Naphthoflavone (β-NF) treatment, displayed transgene recombination and K-*ras*^{Asp12} expression in the murine intestines, but developed few intestinal adenomas over 2 years. However, when crossed with *Apc*$^{Min/+}$ mice, the K-*ras*^{Asp12}/*Cre*/*Apc*$^{Min/+}$ offspring showed acceleration of intestinal tumourigenesis with significantly changed average lifespan ($P < 0.05$) decreased to 18.4 ± 5.4 weeks from 20.9 ± 4.7 weeks (control *Apc*$^{Min/+}$ mice). The numbers of adenomas in the small intestine and large intestine were significantly ($P < 0.01$) increased by 1.5-fold and 5.7-fold, respectively, in K-*ras*^{Asp12}/*Cre*/*Apc*$^{Min/+}$ mice compared with *Apc*$^{Min/+}$ mice, with the more marked increase in adenoma prevalence in the large intestine. To explore possible mechanisms for K-*ras*^{Asp12} and *Apc*^{Min} co-operation, the Mitogen-activated protein kinase (*Mapk*), *Akt* and *Wnt* signalling pathways, including selected target gene expression levels, were evaluated in normal large intestine and large intestinal tumours. K-*ras*^{Asp12} increased activation of *Mapk* and *Akt* signalling pathway targets phospho-extracellular signal-regulated kinase (pErk) and pAkt, and increased relative expression levels of *Wnt* pathway targets vascular endothelial growth factor (*VEGF*), *gastrin*, cyclo-oxygenase 2 (*Cox2*) and T-cell lymphoma invasion and metastasis 1 (*Tiam1*) in K-*ras*^{Asp12}/*Cre*/*Apc*$^{Min/+}$ adenomas compared with that of *Apc*$^{Min/+}$ adenomas, although other *Wnt* signalling pathway target genes such as Peroxisome proliferator-activated receptor delta (*PPARd*), matrix metalloproteinase 7 (*MMP7*), protein phosphatase 1 alpha (*PP1A*) and c-*myc* remained unchanged. In conclusion, intestinal expression of K-*ras*^{Asp12} promotes mutant *Apc*-initiated intestinal adenoma formation *in vivo* more in the large intestine than the small intestine, with evidence of synergistic co-operation between mutant K-*ras* and *Apc* involving increased expression of some *Wnt*-pathway target genes.

Keywords
adenoma, adenomatous polyposis coli, *Cre/LoxP*, intestine, K-*ras*, Min

Received for publication:
24 November 2008
Accepted for publication:
25 February 2009

Correspondence:
Dr Mark J Arends
Department of Pathology
University of Cambridge
Box 235, Addenbrooke's Hospital
Hills Road, Cambridge, CB2 2QQ
UK
Tel.: 01223 217813
Fax: 01223 216980
E-mail: mja40@cam.ac.uk

Colorectal cancers arise following accumulation of mutations or other alterations to several genes, including *Apc* (adenomatous polyposis coli), *β-catenin*, K-*ras*, *Smad* 2 & 4, *PI3k*, *Msh2*, *Mlh1*, *p53* and others, along with large-scale genomic changes and epigenetic alterations (Fearon & Vogelstein 1990; Powell *et al.* 1992; Al-Aynati *et al.* 2004; Arends & Frayling 2005; Sjöblom *et al.* 2006; Wood *et al.* 2007). K-*ras* is mutated in 40–50% of both colorectal adenomas and carcinomas, with codon 12 aspartate as one of the common mutations (Bos *et al.* 1987; Jervoise *et al.* 1998; Andreyev *et al.* 2001). K-*ras* mutations may be found at all stages of colorectal neoplasm development, including dysplastic aberrant crypt foci (ACF) (Shivapurkar *et al.* 1997), hyperplastic polyps (Otori *et al.* 1997), adenomas and carcinomas (Ohnishi *et al.* 1997). K-*ras* mutations are associated with increased size and dysplasia in adenomas, suggesting that they may be permissive for growth disorder early in tumourigenesis (Ohnishi *et al.* 1997). Mutation of the K-*ras* gene reduces or abolishes the protein's intrinsic GTPase activity, locking it in a guanosine triphosphate (GTP) bound conformation that is constitutively active and generates signals to downstream effectors (Barbacid 1987). This activation of *ras* has several effects on rodent fibroblasts cultured *in vitro*, including the establishment of the transformed phenotype, anchorage independent growth, focus formation and tumourigenic potential when injected into animals (Spandidos & Wilkie 1984; Arends *et al.* 1993, 1994), but its roles in colorectal tumour initiation and progression are still incompletely understood.

The *Apc* gene, frequently called the 'gatekeeper' of colorectal cancer, is mutated in 60–80% of sporadic colorectal adenomas and cancers. Inherited *Apc* defects give rise to the syndrome of familial adenomatous polyposis coli (FAP) manifested by the formation of hundreds or thousands of adenomas (Rustgi 1994). Familial adenomatous polyposis coli (FAP) is modelled by the multiple intestinal neoplasia ($Apc^{Min/+}$) mouse, which has one wild-type allele and one *Apc* allele mutated at codon 850, and displays *Apc*-driven tumourigenesis in the intestines (Su *et al.* 1992). Investigation of adenomas from both FAP patients and Min mice (each with one inherited *Apc* gene mutation) has shown either mutation or loss of the wild-type *Apc* allele in most adenomas (Ichii *et al.* 1993; Levy *et al.* 1994). Thus, mutation or loss of both *Apc* alleles represents the most important pathway of adenoma initiation.

K-*ras* and *Apc* mutations both occur during the early stages of colorectal adenoma formation, including dysplastic aberrant crypt foci, early monocryptal adenomas, oligocryptal adenomas as well as established adenomas, and it has been hypothesized that these two mutant genes may co-operate during tumourigenesis. Previously, we showed that induction of intestinal expression of a similar conditional knock-in K-ras^{Val12} transgene can accelerate intestinal tumour formation on a *Msh2*-null background (Luo *et al.* 2007a); however, the precise contributions of mutated K-*ras* to mutant *Apc*-driven intestinal tumourigenesis are insufficiently well characterized. *In vitro* studies have shown synergy between mutant *ras* and *Apc*, as together they promote transformation of colonic epithelial cell lines (D'Abaco *et al.* 1996), but the results of *in vivo* experiments have been contradictory (Johnson *et al.* 2001; Janssen *et al.* 2002, 2005, 2006; Guerra et al. 2003; Tuveson *et al.* 2004; Sansom *et al.* 2006; Calcagno *et al.* 2008; Haigis *et al.* 2008). Oncogenic K-*ras* has been shown to co-operate with mutant *Apc* during tumourigenesis affecting the intestines (Janssen *et al.* 2006; Sansom *et al.* 2006; Haigis *et al.* 2008), but the mechanisms are incompletely understood and the site of maximal co-operation within the small or large intestines is uncertain.

Here, we describe a strain of mice with a conditional mutated K-ras^{Asp12} transgene that when crossed with *Ah-Cre* mice, allows inducible expression of K-ras^{Asp12} in the intestinal epithelial stem cell compartment of the crypts. This model was used to test the effect of mutant K-ras^{Asp12} on intestinal tumourigenesis *in vivo*. In mice carrying a mutant K-ras^{Asp12} transgene and *Ah-Cre*, following induction of recombination and expression of mutated K-ras^{Asp12} in the intestines, only a few small adenomas were found in the small intestine, showing that mutant K-*ras* alone does not significantly initiate tumour formation in the intestine, confirming our previous findings (Luo *et al.* 2007a). The mutant K-ras^{Asp12}/*Ah-Cre* transgenic mice were crossed with $Apc^{Min/+}$ mice and the progeny harbouring mutated K-ras^{Asp12}, *Ah-Cre* and $Apc^{Min/+}$ alleles showed acceleration of intestinal tumourigenesis, with greater effects on the large than the small intestines, and the adenomas showed evidence of synergism between mutant K-*ras* and *Apc* involving increased expression of some *Wnt*-pathway target genes.

Materials and methods

Transgene construction

The K-ras^{Asp12} transgene expression construct was generated as follows: the oncogenic *ras* gene was a previously made chimeric human N/K-*ras* gene (Maher *et al.* 1995), which contained the cDNA sequence encoding amino acids 1–83 from the human N-*ras*, including a mutation in codon 12 coding for an aspartic acid residue (Asp) instead of the wild-type glycine, fused with the cDNA sequence encoding amino acids 84–188 from the human K-*ras* gene that includes exon

4B in continuity with exon 3 (excluding exon 4A). The entire chimaeric *ras* gene encodes the correct primary amino acid sequence for the human K-Ras^{Asp12} 4B protein, because K-Ras and N-Ras proteins share the same amino acid sequence for the first 83 residues. This chimaeric K-*ras*^{Asp12} transgene cDNA fragment was inserted into the Promega vector PCIneo that featured a floxed-'STOP' cassette, constructed as described elsewhere (Brooks *et al.* 2001; James *et al.* 2003; Luo *et al.* 2007a) using the synthetic linker *Not*I – *LoxP* – *Hind*III–*Xho*I – *LoxP* – *Not*I (5′-GGC CGC ATA ACT TCG TAT AGC ATA CAT TAT ACG AAG TTA TAA GCT TAT TTG AGG CTC GAG AAA TAA CTT CGT ATA GCA TAC AT T ATA CGA AGT TAT AGC TGG C-3′) and the neomycin resistance gene containing 'STOP' sequence inserted into the *Hind*III and *Xho*I sites. Upstream of this *lox-STOP-lox* sequence was placed the cytomegalovirus (CMV) promoter and downstream was the K-*ras*^{Asp12} transgene followed by an encephalomyocarditis virus internal ribosome entry site (*IRES*)–enhanced green fluorescent protein (*EGFP*) sequence (Figure 1). This construct was linearized by *Bam*HI, purified by agarose gel electrophoresis with electroelution and injected into fertilized FVB/N mouse oocytes to generate founder mice.

*Genotyping the K-*ras^{Asp12} *mice*

For genotyping, four pairs of primers, located in the sequences for the CMV promoter, neomycin resistance gene, human K-*ras* exon 4B and *EGFP* sequences, were designed and developed (Luo *et al.* 2007a) for PCR assays for rapid screening of the K-*ras*^{Asp12} positive mice (Figure 1). Tail tips of offspring were digested overnight at 55 °C in 500 μl DNA lysis buffer (50 mmol/l Tris-HCl, pH 7.5, 0.1 mol/l NaCl, 0.5% SDS, 5 mmol/l ethylene diamine tetra-acetic acid (EDTA), 100 μg/ml proteinase K). Proteins were precipitated with 6 mol/l NaCl. To precipitate DNA, one volume of isopropanol was added and the mixture centrifuged, the DNA pellet was washed in 70% ethanol and dissolved in 30 μl TE buffer. The quality of genomic DNA samples was estimated by amplifying a wild-type *Apc* gene fragment (Luo *et al.* 2007a). Polymerase chain reaction conditions were 95.0 °C for 30 s, 60.0 °C for 30 s and 72.0 °C for 45 s for 35 cycles.

Genotyping the Apc$^{Min/+}$ *mice*

Apc$^{Min/+}$ mice have a nonsense mutation at codon 850 in the *Apc* gene (Su *et al.* 1992). We designed four pairs of PCR primers to distinguish this point mutation from the wild-type sequence. The first two primer pairs were used under very strict PCR conditions (95.0 °C for 30 s, 66.5 °C for 30 s and 72.0 °C for 45 s for 35 cycles), the primer pair *Apc*1a–*Apc*1b amplified wild-type *Apc* gene fragments, whereas the primer *Apc*2b (which has just one base difference at the 3′ terminus of the primer) was used in the primer pair *Apc*1a–*Apc*2b to amplify the mutant *Apc* sequence. The second two primer pairs were also used under strict PCR conditions (95.0 °C for 30 s, 72.0 °C for 75 s for 35 cycles), the primer pair *Apc*1c–*Apc*1d amplified wild-type *Apc* sequence, whereas the primer *Apc*2d (with just one base difference at the 3′ terminus of the primer) was used in the primer pair *Apc*1c–*Apc*2d to amplify the mutant *Apc* gene sequence. The sequences of PCR primers were as follows: *Apc*1a, 5′ GTT CTC GTT CTG AGA AAG ACA GAA GTT T 3′; *Apc*2b, 5′ GTT CTC GTT CTG AGA AAG ACA GAA GTT A 3′; *Apc*1b, 5′ TCG TTT ATA TTC CAC TTT GGC ATA AGG C 3′; *Apc*1c, 5′ CAA GTC TGC CAT CCC TTC ACG TTA GGA A 3′; *Apc*1d, 5′ CTG AGG CCA ATA CCT CGC TCT CTC TCC A 3′; *Apc*2d, 5′ CTG AGG CCA ATA CCT CGC TCT CTC TCC T 3′. The optimal primer annealing temperatures were determined by testing the primer pairs against known wild-type *Apc* sequences (C57Black6/J or B6 mice) and known *Apc*^{Min} sequences (known Min mice with multiple adenomas and known mutational status proven by DNA sequencing) at a range of annealing temperatures on a gradient PCR block (Figure 1c).

*Real-time quantitative DNA PCR was used to identify the copy number of the K-*ras^{Asp12} *transgene*

To estimate the number of copies of human K-*ras*^{Asp12} transgene integrated into the genome of the K-*ras*^{Asp12} transgenic mice, real-time quantitative DNA PCR (qPCR) was used to amplify K-*ras* sequences from both endogenous murine K-*ras* proto-oncogene (two copies per cell) and the integrated human K-*ras*^{Asp12} transgenes. One pair of primers was designed that bound with identical specificity to both human and mouse K-*ras* exon three sequences: K-*ras* mouse/human exon 3 sense primer: 5′ TTA TTG ATG GAG AAA CCT GTC TCT TG 3′, K-*ras* mouse/human exon 3 antisense primer: 5′ TTA TGG CAA ATA CAC AAA GAA AGC C 3′. Briefly, 100 ng genomic DNA extracted from control B6 mice and from mice containing the K-*ras*^{Asp12} transgene was used for qPCR. The qPCR reactions were amplified using the iCycler (BioRad, Hemel Hempstead, UK) starting with denaturation at 95.0 °C for 3 min, then 35 cycles of 95.0 °C for 15 s and 60.0 °C for 1 min. The specificity of the PCR reactions was determined from the dissociation curve analysis and 2% agarose gel electrophoresis of the products. All PCR products were quantitatively analysed in the linear range of the log-plotted exponential phase of PCR amplification.

The quantity of the specific K-*ras*-derived fragments was obtained from standard curves with normalization using the wild-type *Apc* gene PCR of the same sample. All qPCR reactions were performed in triplicate and the mean (±SD) value of K-*ras* copy number was calculated.

Analysis of transgene recombination at the LoxP *sites by PCR and DNA sequencing*

Genomic DNA was prepared from intestinal tumours and non-tumour-bearing tissue samples by overnight proteinase K digestion, followed by purification using a QIAamp Tissue kit (Qiagen, UK). Transgene recombination was detected by PCR using the primers: sense primer RE-CMV, 5′ TCA GAT CAC TAG AAG CTT TAT TGC GG 3′, which was located in the CMV promoter; antisense primer RE-K-ras^{Asp12}, 5′ TAC AAA GTG GTT CTG GAT TAG CTG GA 3′, which was located in exon 3 of the K-ras^{Asp12} transgene. The PCR primers were used in a PCR assay to detect recombination at the two *LoxP* sites leading to excision of the 'STOP' cassette and joining together of the CMV promoter and the K-ras^{Asp12} transgene. The same PCR primers were used as DNA sequencing primers to sequence the PCR product from both ends by standard Sanger DNA sequencing methods.

Reverse transcription PCR analysis of expression of K-ras^{Asp12} *transcripts*

To induce *Cre* expression via the *Ah* promoter of the *Ah-Cre* transgene, the mice were injected with 160 mg/kg β-naphthoflavone (β-NF) (Sigma, Dorset, UK) dissolved in corn oil for 6 days as described previously elsewhere (Ireland *et al.* 2004; Luo *et al.* 2007a), and controls received either no treatment or corn oil only. Human K-ras^{Asp12} 4B expression was determined using the K-*ras* 4B upstream primer 5′-GTA CCT ATG GTC CTA GTA GGA AAT AAA-3′ located in human K-*ras* exon 3; and the K-*ras* 4B downstream primer 5′-CTG ATG TTT CAA TAA AGG AAT TCC A-3′ located in human K-*ras* exon 4B. The PCR product size was 159 bp. For quantitative RT-PCR, 100 ng of total RNA of different tissue samples was reverse transcribed in 25 ml volume using the iTaq SYBR Green kit RT-PCR kit (BioRad). All RT-qPCR reactions were amplified starting with denaturation at 95.0 °C for 3 min, then 45 cycles of 95.0 °C for 15 s and 60.0 °C for 1 min.

Western blot and immunohistochemical analyses

For Western blot analysis, fresh tissue samples were lysed in protein lysis buffer containing 50 mmol/l Tris–HCl (pH 7.4), 150 mmol/l NaCl, 0.5% NP-40 (Shell Chemical Co., New York, USA) and protease inhibitors. Soluble protein lysates were quantified using the BCA Protein Assay kit (Pierce, Rockford, Illinois, USA). Total proteins were separated by 15% SDS-PAGE, transferred to nitrocellulose membranes (Schleicher and Scheull, UK) and incubated with the corresponding antibodies including anti-K-Ras^{Asp12} (Calbiochem, Merck, Darmstadt, Germany) and anti-*Cre* rabbit polyclonal antibody (Novagen Inc., Madison, Wisconsin, USA). Blots were hybridized with antibodies in 1:1000 dilutions. Visualization was performed with chemiluminescence. The p-Mapk Family (including phospho-extracellular signal-regulated kinase (pErk) 1&2) Rabbit mAb Sampler Kit and the p-Akt Pathway Sampler Kit (Cell Signalling Co., Beverley, Massachusetts, USA) were used for Mapk and Akt pathway protein analysis by both Western blotting and immunohistochemical analyses. Immunohistochemical analysis of selected proteins involved use of goat anti-gastrin polyclonal antibody, rabbit anti-T-cell lymphoma invasion and metastasis 1 (Tiam1) (C-16) polyclonal antibody (both from Santa Cruz Biotechnology Inc., Santa Cruz, California, USA), rabbit anti-cyclo-oxygenase 2 (Cox2) monoclonal antibody, rabbit anti-β-catenin monoclonal antibody, rabbit anti-phospho-GSK-3beta (Glycogen synthase kinase 3beta) monoclonal antibodies and rabbit anti-Vascular endothelial growth factor (VEGF) polyclonal antibody (all from Novus Biologicals Inc., Littleton, Colorado, USA).

For immunohistochemical analysis, immunoperoxidase detection was performed on 4 μm formalin-fixed, paraffin-embedded tissue sections. Sections were deparaffinized in xylene and rehydrated through graded alcohols to distilled water. Antigen retrieval was performed. The anti-phospho-Erk1/2 primary antibodies, anti-phospho-Akt primary antibodies, anti-phosphoGSK-3beta primary antibodies, anti-gastrin primary antibodies, anti-Tiam1 primary antibodies, anti-Cox2 primary antibodies, anti-β-catenin primary antibodies and anti-VEGF primary antibodies were added to the sections and incubated for 1 h at room temperature, followed by biotinylated antibody (Dako, Denmark) and peroxidase-conjugated ExtroAvidin (Sigma-Aldrich, St Louis, Missouri, USA). Finally, 3, 3′-diaminobenzidine tetrahydrochloride (DAB) was used as chromogen (Kem-En-Tec A/S, Denmark). Sections were counterstained with Mayer's haematoxylin. No signal was detected in sections when the primary antibody was omitted as a negative control.

Analysis of tumours

Mice were killed and the number of intestinal tumours counted. The whole intestinal tract of each mouse was

removed, rinsed gently in PBS using a syringe and opened lengthwise. The opened intestine was spread out flat on filter paper. All tumours were counted under a dissecting microscope at 15× magnification, always by the same investigator. The smallest tumours identified were about 0.5 mm in diameter. Some tumours were bisected and half taken fresh for DNA, RNA and protein analyses. The samples were then fixed in 10% neutral-buffered formalin solution. Tumours of the small and large intestines and other tissues were processed for paraffin embedding. Sections were prepared for H&E staining for confirmation of the diagnosis and immunohistochemistry.

Real-time quantitative RT-PCR evaluation of relative expression levels of target genes

Real-time quantitative reverse transcription PCR (real-time RT-qPCR) was carried out to measure the relative expression levels of a range of selected target genes (Table 1 shows the PCR primer sequences) using the comparative cycle threshold (Ct) method as described elsewhere (Luo *et al.* 2007a). The values for *β-actin* were used to normalize the gene expression data. The gene expression levels in intestinal tumours relative to the control intestinal normal tissues were calculated using the following formulas: $\Delta\Delta Ct = \Delta Ct$ test$-\Delta Ct$ control, fold change = $2^{-\Delta\Delta Ct}$.

Statistical and clustering analysis

The SPSS (SPSS, Chicago, Illinois, USA) statistical package was used for all statistical analyses. Student's t-tests were used to compare adenoma numbers, and the Kaplan–Meier survival curve method with log rank test was used to compare mouse survival data following tumour progression and mouse deaths. Unsupervised hierarchical clustering of cases was performed using the Euclidean similarity measure and Ward linkage (Johnson *et al.* 2006) and this was carried out using in-house software written in R (R Development Core Team. R: A language and environment for statistical computing. R Foundation for statistical computing: Vienna, Austria) and visualization was carried out using TREEVIEW 1.6 software (Eisen *et al.* 1998).

Results

*Generation and genotyping of conditional K-*ras^{Asp12} *transgenic mice and analysis of the transgene copy number*

The conditional K-*ras*^{Asp12} transgene is based on chimaeric cDNA sequences for exons 1, 2, 3 and 4B (but not exon 4A and with no introns), allowing expression of a transcript that is translated into a protein with the correct amino acid sequence for the whole of human K-Ras4B protein with a codon 12 aspartate mutation (Maher *et al.* 1995). The structure of the construct was confirmed by restriction enzyme digestion and DNA sequencing (data not shown), its expression and correct functioning were tested *in vitro* in HM1 murine embryonic stem (ES) cells (data not shown and Brooks *et al.* 2001). The K-*ras*^{Asp12} transgene construct was linearized by *BamHI*, purified and microinjected into fertilized FVB/N mouse oocytes. K-*ras*^{Asp12} transgenic founder mice were generated and shown to contain the K-*ras*^{Asp12} transgene (Figure 1) and these were subsequently backcrossed with B6 mice for seven to eight generations until the transgene was on a congenic B6 background. The K-*ras*^{Asp12} positive offspring mice were identified by PCR assays for the presence of CMV promoter, human K-*ras* 4B, neomycin-resistance gene and *EGFP* gene sequences (Figure 1b). The exon 3 DNA sequences of both human and mouse K-*ras* genes are highly homologous, with a DNA sequence difference of only two base pairs. A pair of PCR primers was designed to bind equally to both human and murine K-*ras* exon 3 DNA sequences, and real-time quantitative DNA PCR (qPCR) analysis showed that the relative value of K-*ras* exon 3 mean (±SD) copy number in B6 control mice was 2.00 ± 0.37 ($n = 6$), whereas that in K-*ras*^{Asp12} transgenic mice was 3.80 ± 0.55 ($n = 6$), indicating that B6 control mice have two endogenous copies of K-*ras* and K-*ras*^{Asp12} transgenic mice have 4 copies, including the two normal endogenous murine K-*ras* genes and two copies of the K-*ras*^{Asp12} transgene (Figure 1d).

Genotyping of Apc$^{Min/+}$ *mice*

Apc$^{Min/+}$ mice have a nonsense point mutation at codon 850 in the murine *Apc* gene (Su *et al.* 1992). We designed four pairs of PCR primers to identify this point mutation. Under very strict PCR conditions (with annealing at 66.5 °C), the primer pair *Apc*1a–*Apc*1b amplified the wild-type *Apc* gene sequence, whereas primer *Apc*2b (with just one base difference at the 3′ terminus of primer) in the primer pair *Apc*1a–*Apc*2b amplified the mutant *Apc* gene sequence. Under another set of strict PCR conditions (with annealing at 72.0 °C), the primer pair *Apc*1c–*Apc*1d amplified the wild-type *Apc* gene sequence, whereas primer *Apc*2d (with just one base difference at the 3′ terminus of primer) in the primer pair *Apc*1c–*Apc*2d amplified the mutant *Apc* gene sequence (Figure 1c).

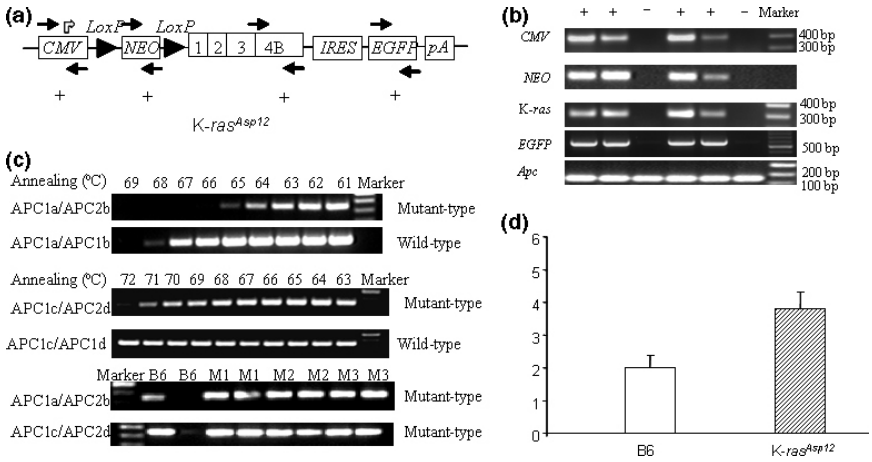

Figure 1 K-*ras*^{Asp12} construct, PCR genotyping and construct copy number assay. (a) Structure of the K-*ras*^{Asp12} transgene: cytomegalovirus (CMV) immediate early promoter; neomycin (*NEO*), resistance gene; 1, 2, 3 and 4B, K-*ras* exons 1, 2, 3 and 4B; encephalomyocarditis virus internal ribosome entry site (*IRES*); enhanced green fluorescent protein (*EGFP*); pA, polyadenylation signal; ▶, 34 bp *LoxP* sites; the positions and orientations of the PCR primers used for genotyping analyses are depicted by arrows (→). (b) Typical results of genotyping PCR assays from offspring of transgenic mice and control (B6) mice. Polymerase chain reaction (PCR) amplification of an *Apc* gene fragment was used as the control for the quality of genomic DNA samples. + represents mouse tail DNA from mice positive for the K-*ras*^{Asp12} transgene; − represents mouse tail DNA from control B6 mice negative for the transgene constructs. (c) Genotyping *Min* mice by allele-specific primers binding either the wild-type or the mutant *Apc* gene sequence. Upper two panels: use of *Apc*1a/*Apc*1b (wild-type *Apc* primer pair) and *Apc*1a/*Apc*2b (mutant *Apc* primer pair) to amplify wild-type B6 genomic DNA, shows that at 66 °C and 67 °C annealing temperatures, wild-type *Apc* can be distinguished from mutant *Apc*. Middle two panels: use of *Apc*1c/*Apc*1d (wild-type *Apc* primer pair) and *Apc*1c/*Apc*2d (mutant *Apc* primer pair) to amplify wild-type B6 genomic DNA, shows that at 72 °C annealing temperature wild-type *Apc* can be distinguished from mutant *Apc*. Lower two panels: an example of the use of both sets of wild-type and mutant *Apc* primer pairs *Apc*1a/*Apc*1b (W) and *Apc*1a/*Apc*2b (M) at 66.5 °C (upper) and *Apc*1c/*Apc*1d (W) and *Apc*1c/*Apc*2d (M) at 72 °C (lower) to amplify genomic tail DNA samples from known negative control B6 (wild-type only) and known Min (M1 to M3, with both wild-type and mutant *Apc* alleles) mice. (d) Bar chart of relative copy numbers of K-*ras* exon 3 sequences (human and mouse) by Real-time quantitative DNA PCR (qPCR), showing the mean (error bar = SD) relative copy number of K-*ras* exon 3 in B6 control mice was 2.00 ± 0.37 (n = 6), and that of K-*ras*^{Asp12} was 3.80 ± 0.55 (n = 6), indicating the presence of two endogenous and two transgenic copies of K-*ras*.

*Conditional recombination and expression of the K-*ras^{Asp12} *transgene in the intestines of K-*ras^{Asp12}/Cre *transgenic mice*

K-*ras*^{Asp12} transgene positive mice were crossed with *Ah-Cre* mice that are capable of transient expression of Cre recombinase protein in the epithelial cells of the intestinal crypts, including the epithelial stem cells, following β-Naphthoflavone (β-NF) intraperitoneal injection (Ireland *et al.* 2004; Luo *et al.* 2007a). This generated offspring mice positive for both conditional K-*ras*^{Asp12} and *Ah-Cre* transgenes, confirmed by PCR-based genotyping assays (Figure 1b). A test group of 25 mice positive for K-*ras*^{Asp12}/*Cre* transgenes were treated with β-NF (160 mg/Kg per day for 6 days) to induce transient expression of Cre recombinase protein in intestinal epithelium.

A PCR assay was used to detect recombination occurring at the two *LoxP* sites (flanking the 'STOP' cassette), which amplified the DNA fragment between the two primers (one situated in the CMV promoter and the other in K-*ras* exon 3), to produce an approximately 500 bp fragment (indicating *LoxP* recombination) amplified from genomic DNA extracted from both small and large intestines and also from stomach, liver and spleen, but not from heart, pancreas or skin (Figure 2). This showed that Cre-mediated recombination at the two *LoxP* sites had occurred to excise the large approximately 2 Kb 'STOP' cassette containing the neomycin-resistance gene, bringing together the CMV promoter sequence and the K-*ras*^{Asp12} sequence. This was confirmed by DNA sequencing of this PCR product which showed that the neomycin-resistance gene containing 'STOP' cassette had been deleted between the two *LoxP* sites (with *NotI* restriction enzyme sites outside of both *LoxP* sites), leaving only one *LoxP* site (flanked by 2 *NotI* sites) between the CMV promoter and adjacent K-*ras* sequence (Figure 2). The sequencing data also confirmed the presence of DNA

Table 1 Polymerase chain reaction primers for expression analysis

Gene	Upstream PCR primer	Downstream PCR primer
Axin	TCTCCGAGACAGAGACAAAATCAC	TCTTGGTTAGCAGCTCCTTGAACT
Apc	TGATACTTCTTCCAAAGCTTTGGCTAT	TCTCGTTCTGAGAAAGACAGAAGCT
β-catenin	CCATTGAAAATATCCAAAGAGTAGC	CTCAGACATTCGGAATAGGACAG
CD44	GCGGTCAATAGTAGGAGAAGGTGT	CTCGTCAGCTGTCATACACTGGT
CMV	TGACGTCAATGGGTGGAGTA	TGCCAAAACAAACTCCCATT
c-myc	AAATCCTGTACCTCGTCCGATTC	ATCAATTTCTTCCTCATCTTCTTGC
Cox2	ACAGACTGTGCCACATACTCAAGC	GATACTGGAACTGCTGGTTGAAAAG
Cyclin D1	TTTCTTTCCAGAGTCATCAAGTGTG	ACCAGCCTCTTCCTCCACTTC
Cyclin D2	GAACTGGTAGTGTTGGGTAAGCTG	GTACATGGCAAACTTGAAGTCG
E-cadherin	TACCCGGGACAATGTGTATTACTAT	GAAGTTTCCAATTTCATCAGGATT
EGFP	GCAAGGGCGAGGAGCTGTTC	CCATGCCGAGAGTGATCCCG
Ephb2	CCATTGAACAGGACTACAGACTACC	CACCGTGTTAAAGCTGGTGTAG
Gastrin	ACCAATGAGGACCTGGAACAG	TGCTAGTCCTACTGGTCTTCCTCA
Igfbp4	CACGAAGACCTCTTCATCATCC	CCTAGTAGGGGGCACTGAGTC
K-*ras* 4B	TCTTAAGGCATACTAGTACAAGTGGT	TTTGTTTCACACCAACATTCA
MMP7	GAGTACTGGACTGATGGTGAGGAC	CATATAACTTCTGAATGCCTGCAA
Neo	TGGAGAGGCTATTCGGCTATGACTGGG	TGGATACTTTCTCGGCAGGAGCAAGGTG
N/K-*ras*	AGTGGTTATAGATGGTGAAACCTGTT	TTGTCTTTGCTGATGTTTCAATAAAA
PP1A	CTACTGTGTGATCTCCTGTGGTCT	AGAAGAGTGTCACCAACTGTCTCTT
P21	CTGTCTTGCACTCTGGTGTCTG	GGCACTTCAGGGTTTTCTCTT
PP2A	GAATGACTACACTCTTCTGCATCAA	TATCAAGAATGGGTCCTATCTTCTG
P70S6K	ATCTGAAGAGGATGTGAGTCAGTTT	TGTTCGTGGACTACCAATAAATCTT
Pem	GAGTCAAGGAAGACTCGGAAGA	GGCCTTTTCCTCCATTTAATTC
PPARd	CAAGTTCGAGTTTGCTGTCAAGTT	GACCTGCAGATGGAATTCTAGAGC
TCF-4	ACCATGTTGATCACAGACACCAA	GCTGCAGGTGCTGGATGTT
Tcl-1	CAAGAGTAATGAAAAATTCCAGGTG	GATATGGTACAGGATCTGCCAATAC
Tiam1	AATTGTCCACGTGAAATCAGAGT	CTTTAAGCGCACACAATCTCTTG
Trap1a	AAGAATTGGAGAACCTGATGGA	GGGTCGTGGAAGAAATAAATCA
UPA	ATCTTGCACGAATACTACAGGGAAG	CAGTGATCTCACAGTCTGAACCAAA
VEGF	GGAGTACCCCGACGAGATAGAGTA	GAAGCTCATCTCTCCTATGTGCTG

sequence encoding aspartate (in K-*ras*^{Asp12}/*Cre* transgenic mice) at codon 12 (substituted for the wild-type glycine) (Figure 2c).

Reverse transcription polymerase chain reaction (RT-PCR) analysis confirmed the expression of human K-*ras* 4B transcripts in the small and the large intestine and also in some other tissues (stomach, spleen and liver), but not in heart, in K-*ras*^{Asp12}/*Cre* mice (but not in K-*ras*^{Asp12} transgenic mice that were negative for *Cre* or in *Cre* only mice or control B6 mice) after β-NF treatment (Figure 3a).

Phenotypic changes in K-ras^{Asp12}/Cre *mice*

After treatment with β-NF, the only phenotypic changes detected in the intestines were two adenomas in the small intestine and two adenomas in the large intestine in the group of 25 K-*ras*^{Asp12}/*Cre* mice over 2 years, along with one sarcoma and two lymphomas, but these differences were not statistically significant from the control group of B6 mice (n = 16) or Cre-only mice (n = 29) (treated in the same way) over the same 2-year period. Thus, intestinal expression of mutant K-*ras*^{Asp12} alone is not sufficient to significantly initiate intestinal adenomagenesis.

Phenotypic changes in K-ras^{Asp12}/Cre/Apc$^{Min/+}$ *mice*

Apc$^{Min/+}$ mice on a B6 background typically develop 30–50 intestinal adenomas/mouse in the first 6 months of life. To assess the effect of mutated K-*ras* on intestinal tumourigenesis initiated by mutant *Apc*, we crossed K-*ras*^{Asp12}/*Cre* mice with *Apc*$^{Min/+}$ mice to generate a cohort of compound K-*ras*^{Asp12}/*Cre*/*Apc*$^{Min/+}$ mice (n = 25). Four weeks after birth, 160 mg/kg β-NF was injected intraperitoneally for 6 days. A control cohort of *Apc*$^{Min/+}$ mice and *Apc*$^{Min/+}$/*Cre* mice (n = 29) were also treated in the same way. Some of the

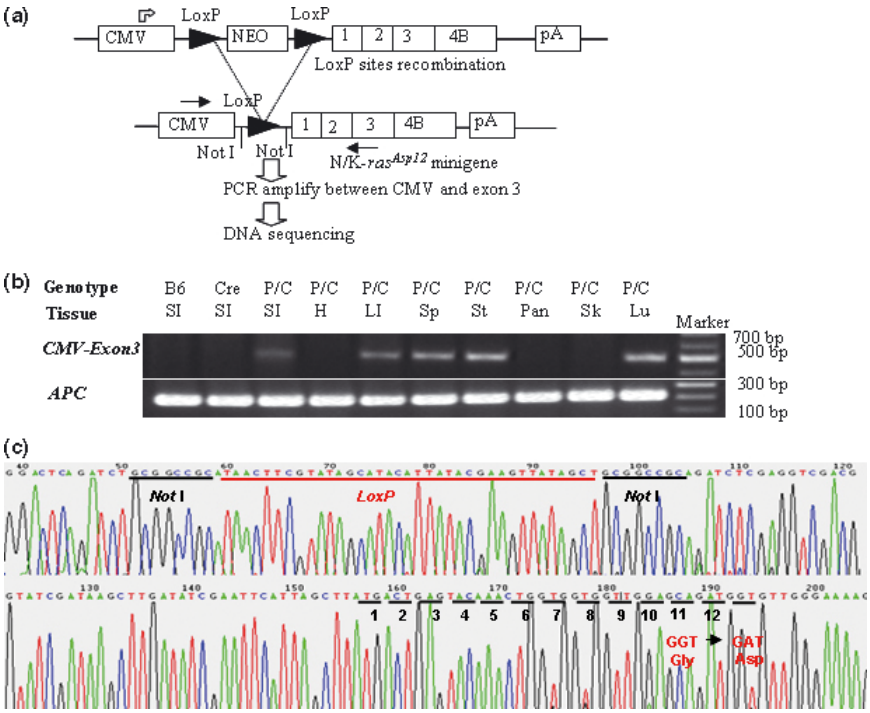

Figure 2 Analysis of conditional K-*ras*^{Asp12} transgene recombination. (a) Schematic representations of the K-*ras*^{Asp12} construct undergoing recombination (after treatment with β-NF to induce *Cre* expression) at the two *LoxP* sites to bring about expression of K-*ras*^{Asp12} transcripts. Without *Cre* recombinase expression, the K-*ras*^{Asp12} transgenes remain silent due to the presence of the neomycin (*NEO*) containing 'STOP' cassette. Upon *Cre*-mediated recombination of the *LoxP* sites (arrowheads), the K-*ras*^{Asp12} transgene is placed directly under the control of the cytomegalovirus (CMV) promoter. Position and orientation of the polymerase chain reaction (PCR) primers used for analysis are depicted by arrows (→). (b) PCR amplification of the DNA fragment between the CMV promoter and K-*ras*^{Asp12} exon 3 generated a 500-bp fragment from genomic DNA extracted from the intestines and some other tissues. B6, Black6 wild-type; C, *Cre*-only genotype; K/C, K-*ras*^{Asp12}/*Cre* genotypes; SI, small intestine; LI, large intestine; Sp, spleen; St, stomach; Pan; pancreas; Sk, skin; Liv, liver; H, heart. (c) DNA sequencing traces of the 500-bp amplified products showed that the 'STOP' cassette had been deleted and there was only one *LoxP* site (flanked by two *Not*I restriction enzyme sites) between the sequences of the CMV promoter and K-*ras* exon 1, with the appropriate codon 12 mutation for the transgene construct: codon 12 GAT in the K-*ras*^{Asp12} mouse intestine.

Apc$^{Min/+}$ mice developed a few colonic adenomatous tumours, but most of the adenomas of the gastrointestinal tract were found in the small intestine as expected. The compound mutant transgenic offspring showed significantly reduced survival ($P < 0.05$ by log rank test) due to multiple intestinal adenoma formation (Figure 4), with bowel obstruction and/or haemorrhage. The average lifespan was decreased from 20.9 ± 4.7 weeks (mean ± SD in *Apc*$^{Min/+}$ mice) to 18.4 ± 5.4 weeks (in K-*ras*^{Asp12}/*Cre*/*Apc*$^{Min/+}$ mice, $P < 0.05$), and no sex differences were observed (Figure 4). The number of duodenal tumours increased from 4.5 ± 1.99 (in *Apc*$^{Min/+}$ mice) to 7.2 ± 3.04 (in K-*ras*^{Asp12}/*Cre*/*Apc*$^{Min/+}$ mice, $P < 0.01$); the number of jejunal tumours increased from 17.9 ± 6.96 (in *Apc*$^{Min/+}$ mice) to 27.2 ± 8.05 (in K-*ras*^{Asp12}/*Cre*/*Apc*$^{Min/+}$ mice, $P < 0.01$); the number of ileal tumours increased from 9.7 ± 3.51 (in *Apc*$^{Min/+}$ mice) to 15.3 ± 3.45 (in K-*ras*^{Asp12}/*Cre*/*Apc*$^{Min/+}$ mice, $P < 0.01$). Thus, there was a 1.5-fold increase in total numbers of small intestinal adenomas in the K-*ras*^{Asp12}/*Cre*/*Apc*$^{Min/+}$ mice. The number of proximal colonic adenomas increased from 0.22 ± 0.48 (in *Apc*$^{Min/+}$ mice) to 1.56 ± 0.99 (in K-*ras*^{Asp12}/*Cre*/*Apc*$^{Min/+}$ mice, $P < 0.01$); the number of distal colonic adenomatous tumours increased from 0.41 ± 0.68 (in *Apc*$^{Min/+}$ mice) to 2.04 ± 1.66 (in K-*ras*^{Asp12}/*Cre*/*Apc*$^{Min/+}$ mice, $P < 0.01$). Thus, compared with *Apc*$^{Min/+}$ mice, there was a 5.7-fold increase in total numbers of large intestinal adenomas in the K-*ras*^{Asp12}/*Cre*/*Apc*$^{Min/+}$ mice (Figure 4). Histological examination confirmed the presence of closely similar adenomas with low grade dysplasia in both the test and control cohorts, and no invasive carcinomas were identified. In the control *Apc*$^{Min/+}$ group, 22 large intestinal tumours were measured for

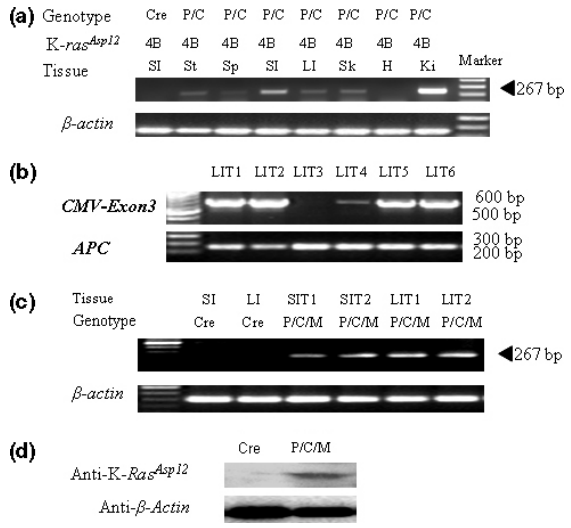

Figure 3 Expression of K-*ras*^{Asp12} in intestinal tissues and tumours. (a) Reverse transcription polymerase chain reaction (RT-PCR) analysis of the expression of K-*ras*^{Asp12} 4B transcripts in different tissues of K-*ras*^{Asp12}/*Cre* transgenic mice, 10 days after completion of the β-NF treatment. C, *Cre*-only genotype, K/C, K-*ras*^{Asp12}/*Cre* genotypes; LI, large intestine; SI, small intestine; St, stomach; Sp, spleen; Sk, skin and Liv, liver as described previously. (b) PCR amplification of a 500-bp DNA fragment between the recombined CMV promoter and K-*ras*^{Asp12} exon 3 from genomic DNA of large intestinal tumours (LIT) from K-*ras*^{Asp12}/*Cre*/*Apc*$^{Min/+}$ transgenic mice treated with β-NF (*Apc* amplification as control). (c) RT-PCR analysis of the expression of K-*ras*^{Asp12} 4B transcripts in two small intestinal tumours (SIT) and two LIT from K-*ras*^{Asp12}/*Cre*/*Apc*$^{Min/+}$ (K/C/M) mice after treatment with β-NF (β-*actin* RNA expression as normalization reference). (d) Western blot analysis of the expression of mutant K-Ras^{Asp12} protein in a large intestinal tumour of a K-*ras*^{Asp12}/*Cre*/*Apc*$^{Min/+}$ (K/C/M-LIT) mouse after β-NF treatment (β-actin protein expression as control) compared with a *Cre*-only mouse large intestine (C-LI).

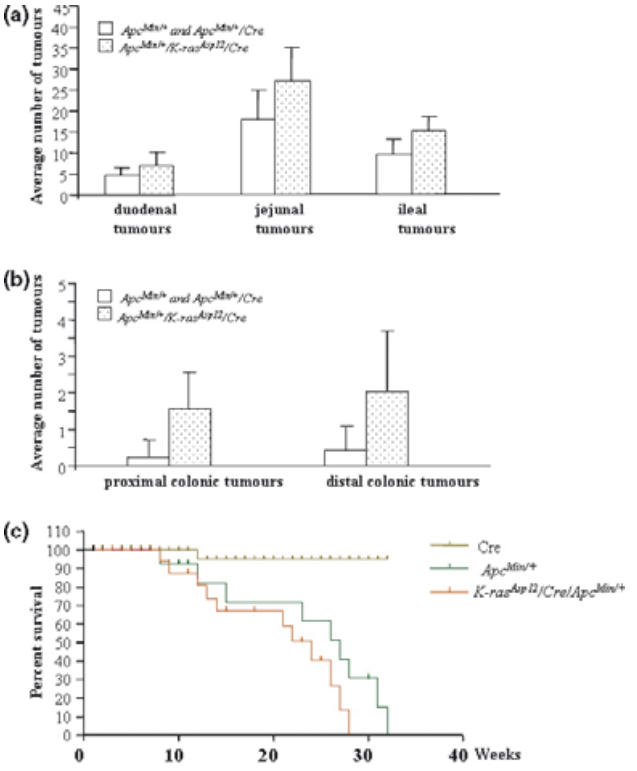

Figure 4 Intestinal tumour prevalence and lifespan in *Apc*$^{Min/+}$ mice and K-*ras*^{Asp12}/*Cre*/*Apc*$^{Min/+}$ mice. (A & B) Average numbers of small intestinal tumours (a) and large intestinal tumours (b) in K-*ras*^{Asp12}/*Cre*/*Apc*$^{Min/+}$ mice (speckled bars), compared with control *Apc*$^{Min/+}$ and *Apc*$^{Min/+}$/*Cre* mice (open bars). (c) Kaplan–Meier survival curves of *Cre* mice (n = 29), *Apc*$^{Min/+}$ (n = 29 in total, including 21 *Apc*$^{Min/+}$ and 8 *Apc*$^{Min/+}$/*Cre* mice), and K-*ras*^{Asp12}/*Cre*/*Apc*$^{Min/+}$ mice (n = 25). Ages of the animals at death (or when killed, if moribund) are given in weeks (*X*-axis).

tumour size: 14 tumours measured 1–2 mm in diameter and eight tumours measured 2–4 mm in diameter (36.4% tumours measured ≥ 2 mm). For the test cohort of K-*ras*^{Asp12}/*Cre*/*Apc*$^{Min/+}$ mice, 49 large intestinal tumours measured 1–2 mm in diameter and 36 measured 2–4 mm in diameter (42.4% tumours measured ≥ 2 mm, with no significant difference between the two groups). However, two tumours in the K-*ras*^{Asp12}/*Cre*/*Apc*$^{Min/+}$ group were more than 4 mm in diameter.

*Analysis of intestinal adenomas for transgene recombination and expression of K-*ras^{Asp12}

To determine the proportion of intestinal adenomatous tumours in which K-*ras*^{Asp12} transgene recombination and expression occurred following β-NF treatment of the K-*ras*^{Asp12}/*Cre*/*Apc*$^{Min/+}$ mice, a sample of large intestinal tumours (LITs) and small intestinal tumours (SITs) were tested for evidence of transgene recombination by PCR (using the same assay as described above) and K-*ras*^{Asp12} transcript and protein expression (by RT-PCR analysis as described earlier and by Western blot analysis). Genomic DNA analysis showed that K-*ras*^{Asp12} transgene recombination occurred in 23 of 25 (92%) LITs from K-*ras*^{Asp12}/*Cre*/*Apc*$^{Min/+}$ mice (Figure 3b). Those tumours taken from the K-*ras*^{Asp12}/*Cre Apc*$^{Min/+}$ mice with transgene recombination demonstrated expression of K-*ras*^{Asp12} 4B transcripts by RT-PCR analysis. Western blot analysis using specific anti-K-Ras^{Asp12} protein antibody confirmed expression of mutant K-Ras protein in these LIT from β-NF treated K-*ras*^{Asp12}/*Cre*/*Apc*$^{Min/+}$ mice (Figure 3d).

*Effects on target gene expression of the K-*ras/Mapk/Akt *and* Wnt *signalling pathways*

Previous studies have shown that when mutant K-*ras*^{Val12} transgene was introduced into either mouse embryonic stem cells or K-*ras*^{Val12}/*Cre*/*Msh2*$^{-/-}$ transgenic mice, the expression of human K-*ras*^{Val12} was associated with changes in the expression of a range of gene transcripts and proteins, including stem cell-associated genes, such as *Pem*, *Tcl-1* and *Trap*, and with increased phosphorylation of *Mapk* and *Akt* pathway proteins, such as pErk1&2 and pAkt (Luo *et al.* 2007a,b). Here, we used both immunohistochemistry, to show differences in target gene product expression in adenomas (Figure 5), and real-time quantitative reverse transcription PCR assays (Tables 1 and 2), to compare the relative RNA expression levels of a selected panel of genes between non-tumour-bearing normal large intestine (LI) and LITs of β-NF treated *Cre* mice, K-*ras*^{Asp12}/*Cre* mice, K-*ras*^{Asp12}/*Cre*/*Apc*$^{Min/+}$ mice and *Apc*$^{Min/+}$ control mice. Compared with the *Ah-Cre* control mice LI, target genes of the *Mapk* signalling pathway, such as *VEGF*, *Cox2*, *Trap*, *p70S6K* and *cyclinD2*, showed significant increases in relative expression levels by real-time qRT-PCR in the normal colonic tissues of K-*ras*^{Asp12}/*Cre* mice. Normal LI from *Apc*$^{Min/+}$ mice showed a significant increase in relative expression levels of *Cox2*, *uPA*, *Trap* and *β-Catenin* compared with that in the normal LI tissues of *Cre* mice. In large intestinal tumours from *Apc*$^{Min/+}$ mice, there were significant increases in the relative expression levels of *CD44*, *p70S6K* and *gastrin*. Compared with *Apc*$^{Min/+}$ mice LITs, the LITs from K-*ras*^{Asp12}/*Cre*/*Apc*$^{Min/+}$ mice showed significant increases in *CD44* (1.6-fold), *cyclinD2* (4.8-fold), *gastrin* (5.7-fold),

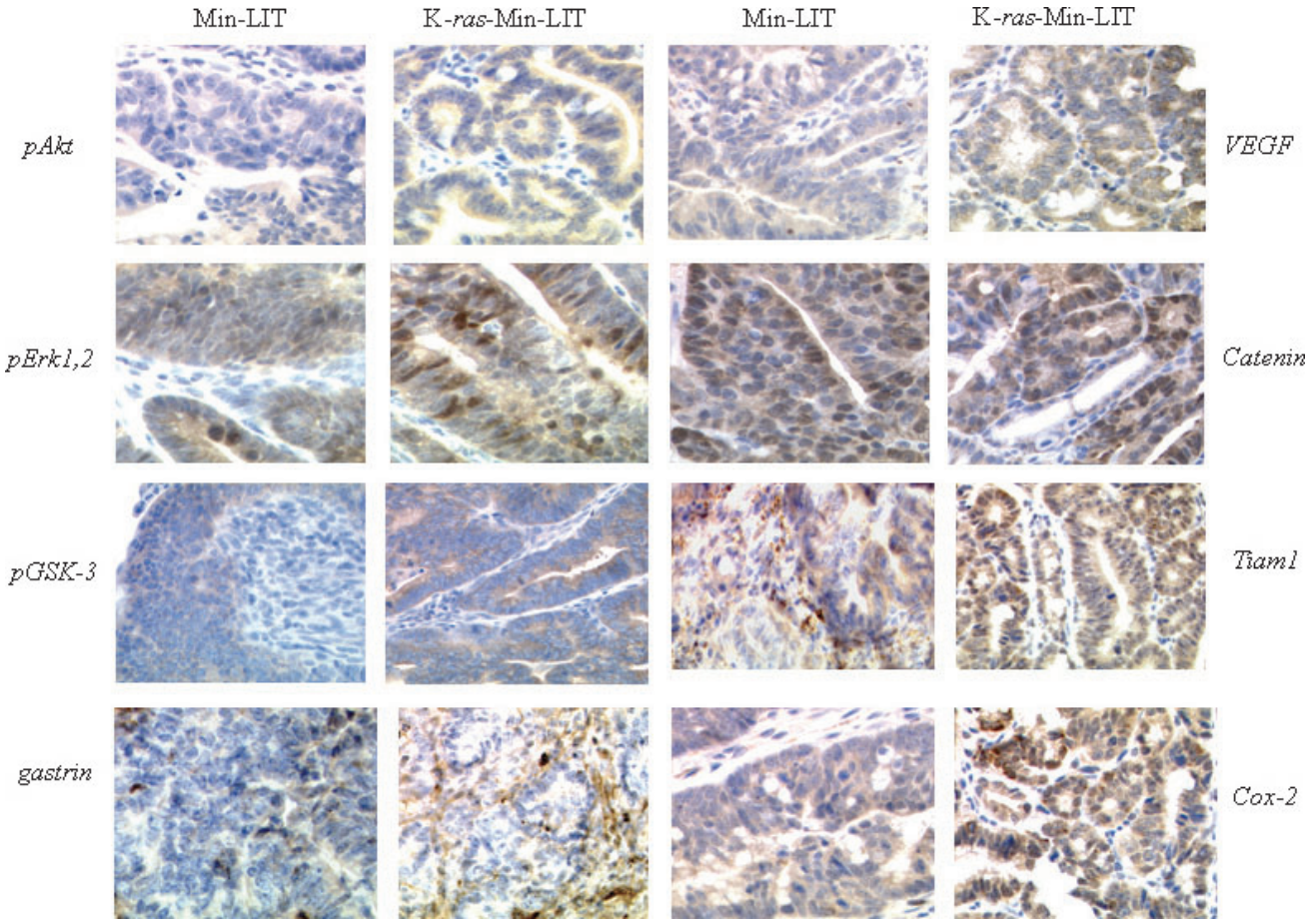

Figure 5 Immunohistochemical analysis of intestinal adenomas. Large intestinal tumours from *Apc*$^{Min/+}$ mice (Min-LIT) and from K-*ras*^{Asp12}/*Cre*/*Apc*$^{Min/+}$ transgenic mice (K-*ras*-Min-LIT) were analysed immunohistochemically for expression of *pAkt*, *pErk 1*, *2*, *pGSK*, *gastrin*, *VEGF*, *β-catenin*, *Tiam1* and *Cox2*.

Table 2 Relative expression levels for selected genes by real-time quantitative reverse transcription polymerase chain reaction

Gene	C LI Ave (3)	C LI SD	K/C LI Ave (3)	K/C LI SD	K/C *vs.* C LI *t*-test	M LI Ave (3)	M LI SD	M *vs.* C LI *t*-test	M LIT Ave (4)	M LIT SD	M-LIT *vs.* M-LI *t*-test	K/C/M LIT Ave (5)	K/C/M LIT SD	K/C/M-LIT *vs.* M-LIT *t*-test
CD44	1.52	0.66	3.53	1.11	0.091	1.21	0.22	0.182	2.54	0.52	**0.005**	4.05	1.52	**0.050**
cyclin D2	1.06	0.59	2.65	0.18	**0.024**	2.75	1.50	0.124	3.39	2.65	0.364	16.42	4.51	**0.001**
PP1A	1.12	0.27	1.90	1.18	0.156	2.34	2.15	0.230	2.90	1.91	0.366	3.51	2.37	0.344
PP2A	0.88	0.10	2.70	1.45	0.085	1.38	0.94	0.206	3.21	1.38	0.053	3.57	1.37	0.354
Axin-2	1.80	0.71	1.98	0.85	0.406	2.16	0.99	0.372	2.52	0.46	0.274	4.35	2.08	0.066
p70S6K	0.95	0.34	3.37	1.24	**0.039**	0.69	0.13	0.117	4.34	2.69	**0.035**	6.32	3.45	0.189
E-cadherin	1.56	0.66	2.34	1.045	0.174	2.78	1.45	0.060	3.16	2.68	0.418	6.79	3.67	0.072
p21	1.51	0.46	1.41	1.66	0.453	3.07	1.25	0.055	3.04	2.84	0.495	3.76	3.38	0.373
Igfbp4	1.39	0.96	2.19	1.62	0.294	3.08	2.49	0.117	2.56	1.27	0.365	10.70	12.57	0.122
Cox2	0.89	0.11	2.73	0.54	**0.011**	3.73	1.23	**0.033**	5.65	3.83	0.226	13.46	10.67	0.105
TCF-4	1.03	0.31	1.48	0.65	0.241	1.74	1.03	0.117	1.64	1.03	0.450	1.77	0.96	0.422
uPA	1.42	0.52	2.79	0.55	0.075	1.90	0.77	**0.043**	4.47	4.12	0.173	7.91	2.45	0.081
gastrin	0.93	0.50	0.73	0.29	0.301	0.96	0.19	0.471	1.58	0.40	**0.030**	8.41	6.81	**0.044**
VEGF	0.98	0.05	2.02	0.43	**0.032**	1.50	0.47	0.091	1.68	0.26	0.269	4.65	1.42	**0.002**
Tiam1	1.18	0.92	1.16	0.15	0.484	1.34	1.12	0.256	3.74	3.40	0.151	3.74	3.87	0.500
cyclin D1	0.85	0.17	0.88	0.24	0.432	1.98	0.87	0.099	3.76	2.00	0.108	2.02	1.09	0.069
MMP7	0.60	0.41	1.86	0.97	0.090	0.67	0.46	0.074	1.24	0.77	0.157	1.28	0.72	0.468
c-Myc	1.10	0.70	1.72	0.47	0.123	1.76	1.27	0.127	3.35	2.97	0.217	3.37	2.24	0.495
PPARd	1.46	0.97	1.21	0.24	0.375	1.72	1.36	0.211	1.13	0.56	0.227	1.73	1.13	0.183
Eph	1.12	0.57	0.79	0.17	0.231	2.06	1.63	0.152	3.79	3.16	0.216	2.35	1.42	0.194
Pem	1.31	1.08	2.11	2.12	0.335	2.12	1.51	0.171	1.87	1.44	0.417	18.95	12.66	**0.017**
Tcl 1	1.77	1.81	3.39	3.71	0.311	1.28	1.26	0.131	2.33	1.25	0.162	15.87	10.17	**0.017**
Trap	0.69	0.27	5.85	3.05	**0.050**	1.90	0.31	**0.007**	0.93	0.84	0.060	17.81	6.45	**0.001**
β-catenin	0.93	0.08	1.12	0.29	0.228	2.65	0.85	**0.031**	2.67	0.43	0.479	2.51	0.58	0.328

Note abbreviations: C, *Cre* genotype; K/C, K-*ras*^{Asp12}/*Cre* genotype; M, *Apc*$^{Min/+}$ genotype; K/C/M, K-*ras*^{Asp12}/*Cre*/*Apc*$^{Min/+}$ genotype; LI, large intestine; LIT, large intestinal tumour; Ave, average value; (n), number of samples analysed given in brackets; *t*-test, Student's *t*-test; *P* value; statistically significant Student's *t*-test *P* values highlighted in bold.

VEGF (2.8-fold), *Pem* (10-fold), *Tcl-1* (6.8-fold) and *Trap* (19-fold). Immunohistochemistry confirmed mild increases in protein expression of *gastrin* and *VEGF* genes in the LITs from K-*ras*^{Asp12}/*Cre*/*Apc*$^{Min/+}$ mice compared with those of *Apc*$^{Min/+}$ mice, and suggested small increases in expression of *Cox2*, *β-Catenin* and *Tiam1*. Immunohistochemical staining confirmed increased expression of the phosphorylated forms of the downstream phosphoprotein effectors of the *Mapk* and *Akt* signalling pathways, including pErk1&2 and pAkt, in the LITs of K-*ras*^{Asp12}/*Cre*/*Apc*$^{Min/+}$ mice compared with those of *Apc*$^{Min/+}$ mice, but little of evidence of changed expression of pGSK-3beta (Figure 5). Hence, there was evidence of activation of both *Mapk* and *Akt* signalling pathways in the LITs of K-*ras*^{Asp12}/*Cre*/*Apc*$^{Min/+}$ mice as well as up-regulation of certain other gene targets of the *Wnt/Apc* pathway.

Hierarchical cluster analysis of the relative expression level data determined by real-time qRT-PCR for the selected target genes showed that the 24 genes were differentially expressed in the normal LI tissues from *Cre* mice, K-*ras*^{Asp12}/*Cre* mice, *Apc*$^{Min/+}$ mice and K-*ras*^{Asp12}/*Cre*/*Apc*$^{Min/+}$ mice and in the large intestinal tumours (LITs) of *Apc*$^{Min/+}$ mice and of K-*ras*^{Asp12}/*Cre*/*Apc*$^{Min/+}$ mice, and that there was clear evidence of clustering broadly together of expression patterns in LI tissues and LITs from mice of the same genotypes (Figure 6). Taken together with the relative expression levels, these cluster patterns indicate that expression of mutated K-*ras* within mutant *Apc*-initiated large intestinal tumours consistently and selectively modulated the expression levels of certain target genes in both the K-*ras/MapK/Akt* and the *Wnt/Apc* pathways.

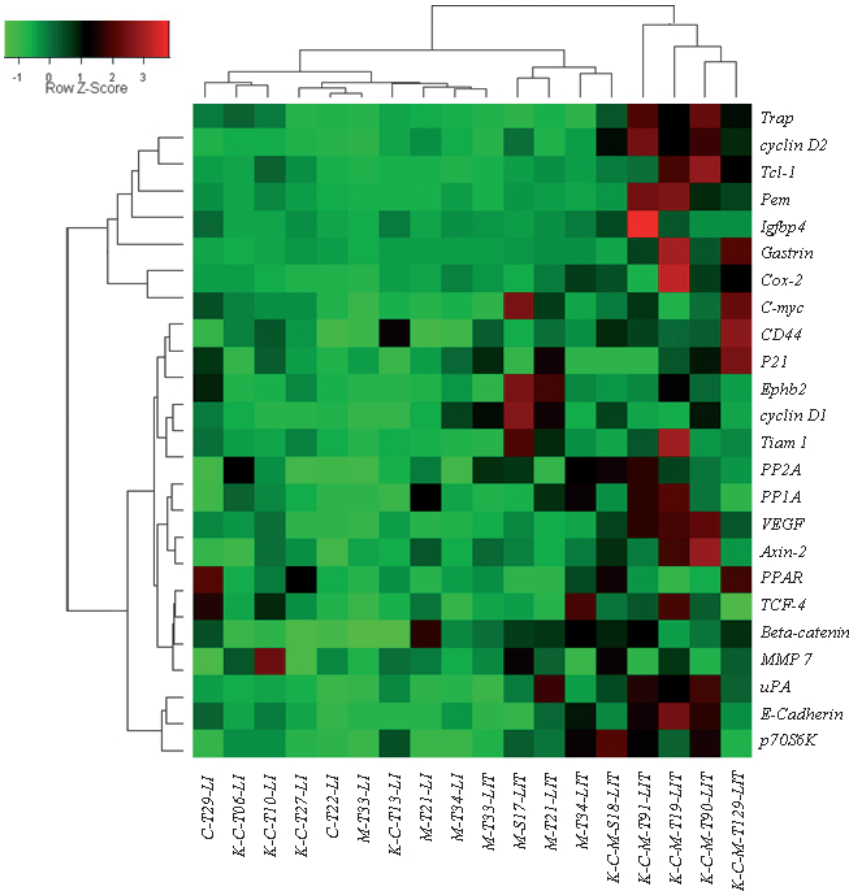

Figure 6 Hierarchical cluster analysis of the differential expression patterns of 24 genes in normal colon and large intestinal tumours. Normal large intestine (LI) tissues from *Cre* (C), K-*ras*^{Asp12}/*Cre* (K-C) and *Apc*$^{Min/+}$ (M) mice and large intestinal tumours (LIT) from *Apc*$^{Min/+}$ (M) and K-*ras*^{Asp12}/*Cre*/*Apc*$^{Min/+}$ (K-C-M) mice were analysed for the relative expression levels of 24 selected genes by real-time quantitative reverse transcription polymerase chain reaction (see Table 2): red represents marked overexpression; dark red/black represents mild over-expression and green represents unchanged or mildly decreased expression levels, with the fold-change shown according to the colour key of the row-Z score. T numbers refer to individual samples. There is a pattern of clustering broadly together of LI tissues and LITs from mice of the same genotypes indicating mostly consistent gene expression changes.

Discussion

Human colorectal neoplasia involves transitions from normal to adenoma to carcinoma associated with accumulation of genetic and epigenetic changes in a multistep process, including activation of K-*ras* by somatic mutation within one or a small number of stem cells located in the intestinal crypt (Fearon *et al.* 1987; Wood *et al.* 2007). K-*ras* mutations have been found in aberrant crypt foci (ACF), early and established adenomas, as well as in cancer-predisposed morphologically normal colon (Morris *et al.* 1996; Malumbres & Barbacid 2003). Aberrant crypt foci (ACF) have been shown to contain K-*ras* mutations, with little or no evidence for mutations in either *Apc* or its downstream effector *β-catenin* (Takayama *et al.* 2001). Several attempts have been made to develop murine models of mutated K-*ras* to investigate the role of K-*ras* mutation in the development of intestinal neoplasia, with variable and contradictory results. Transgenic expression of mutant K-*ras*^{Val12} in the small intestine in post-mitotic villus enterocytes under the control of the rat liver fatty acid binding protein gene 1 (*Fabp1*) promoter caused intestinal dysplasia, but the authors did not observe any tumours, with mutant K-*ras* expressed in cells of the villus which are exfoliated every 2–3 days, thereby quickly eliminating these mutant cells before tumourigenesis can occur (Kim *et al.* 1993). Johnson *et al.* (2001) used a transgenic model, in which the recombinational activation of the mutant K-*ras* was generated at random by recombination occurring within the manipulated allele and these mice were predisposed to a

range of tumour types, predominantly early onset lung cancer, but the transgenic mice failed to develop intestinal tumours. According to the authors, this may have been due either to tissue-specific differences in the frequency of recombination events, or to the relative order of *ras* gene mutations in the course of intestinal tumourigenesis (Johnson *et al.* 2001). Janssen *et al.* (2002) constructed mice with a mutated K-*ras* gene associated with the regulatory region of the murine *villin* promoter, and these *villin*-K-ras^{Val12} mice developed just two tumours over 6 months (Janssen *et al.* 2002), but the *villin* promoter is active during murine embryonic development (Robine *et al.*, 1985; Ezzell *et al.* 1989). Crossing these *villin*-K-ras^{Val12} mice (with constitutive expression of human K-ras^{Val12} 4B isoform) with Apc^{1638N} mice on a crossbred background resulted in intestinal adenoma formation with some carcinomas and there was evidence of Erk activation, but not Akt activation in intestinal epithelium (Janssen *et al.* 2006). Sansom *et al.* (2006) showed that mice with inducible expression (*via Ah-Cre*) of endogenous K-ras^{Val12} 4A and 4B isoforms, when crossed with Apc^{fl580} mice on a crossbred background, developed intestinal adenomas with some carcinomas, with some focal Erk activation. Whereas Haigis *et al.* (2008) showed that mice with constitutive expression (*via Fabpl*-Cre) of endogenous K-ras^{Asp12} 4A and 4B isoforms, when crossed with Apc^{2lox14} mice on a crossbred background, also formed intestinal adenomas with some carcinomas, but with no evidence of Erk activation. However, Calcagno *et al.* (2008) suggested that K-ras^{Asp12} may initiate intestinal neoplasia more in the proximal colon, with some evidence of increased Erk signalling.

To address the questions whether activated K-ras^{Asp12} is able to initiate intestinal tumour formation or rather depends on previous mutations of the 'gatekeeper' gene *Apc*, and whether such oncogenic activity is greater in the small or large intestines, we used a *Cre/LoxP*-based transgenic system with expression of the *Cre* recombinase under control of the *Ah* promoter, which allows activation of *Cre* expression in the adult intestinal crypt stem cells with precise spatial–temporal control (Ireland *et al.* 2004). Using K-ras^{Asp12}/*Cre* mice treated with βNF to trigger Cre-mediated recombination and expression of mutated K-ras^{Asp12} in small and large intestinal epithelium, we found that only two of 25 mice developed adenomas in the intestines over 2 years and, therefore, the K-ras^{Asp12} mutation alone did not significantly initiate adenoma formation in the intestines. A very small (and non-significant) number of sarcomas and lymphomas also developed in other tissues. There may have been a very low frequency of sporadic 'leaky' activation of the *Ah-Cre* transgene leading to Cre recombinase expression and *LoxP* site recombination to trigger mutant K-*ras* expression as a rare event in connective tissue or lymphoid stem cells. However, the small and large intestines were demonstrated to express mutated K-ras^{Asp12}, but appeared unable to initiate intestinal tumour formation as this may require other (possibly multiple) spontaneous mutations in addition. This is consistent with the hypothesis that a contribution from activated K-*ras* to intestinal tumour progression may not occur without the requirement of mutations to other tumour suppressor genes, such as *Apc* (Janssen *et al.* 2006; Sansom *et al.* 2006; Haigis *et al.* 2008).

It is generally accepted that adenomas develop in the intestines of patients with FAP or in Min mice when an appropriate cell acquires a somatic mutation or deletion of the wild-type *Apc* allele to accompany the pre-existing germ-line *Apc* mutation. A polyclonal model of adenoma formation has also been suggested. Although the initiating role of *Apc* mutation is part of most models of colorectal tumourigenesis, it is not clear whether bi-allelic *Apc* mutations are sufficient for the growth of early lesions to form established colorectal adenomas or whether there is a requirement for mutations at other loci, such as K-*ras* (Chen *et al.* 2004). Sansom *et al.* (2006) and Haigis *et al.* (2008) have shown synergistic co-operation between mutant K-*ras* and mutant *Apc* in kidney tumour formation as well as in intestinal tumourigenesis.

Here, we have shown that when *Ah-Cre*-mediated activation of expression of mutated K-*ras* is targeted to the adult intestinal crypt epithelial stem cells, K-ras^{Asp12} does accelerate intestinal adenoma formation on a background of inherited *Apc* mutation and the offspring bearing K-ras^{Asp12}/*Cre*/$Apc^{Min/+}$ mutations showed decreased survival with significant reductions in the average lifespan and significant increases in the numbers of both small (1.5-fold) and large (5.7-fold) intestinal adenomas, with the higher increase seen in the number of large intestinal tumours, more closely mimicking the human situation. Thus, this evidence shows that mutated K-ras^{Asp12} drives progression, but not initiation, of intestinal adenoma formation with greater effects on the large intestine.

Expression analysis of the large intestinal tumours from the K-ras^{Asp12}/*Cre*/$Apc^{Min/+}$ mice, by both immunohistochemistry and real-time quantitative RT-PCR, showed that mutant K-ras^{Asp12} modulates the expression of some target genes of the *Mapk*, *Akt* and *Wnt* pathways. There is immunohistochemical evidence of increased expression of the phosphorylated forms of the downstream effectors of the *Mapk* and *Akt* signalling pathways, including pErk1&2 and pAkt, in the LITs of K-ras^{Asp12}/*Cre*/$Apc^{Min/+}$ mice

compared with those of $Apc^{Min/+}$ mice, confirming activation of both *Mapk* and *Akt* signalling pathways in these tumours. Immunohistochemistry also suggested a mild increase in expression of *β-catenin* protein, with no significant changes in transcript levels, indicating post-translational regulation of protein levels. Mutant K-*ras* has previously been shown to induce the activity of a T cell factor 4 (*Tcf-4*) reporter construct in Caco-2 and HeLa cells, leading to stabilization of the levels of nuclear *β-catenin* and the formation of nuclear *β-catenin/Tcf-4* complexes. Mutant K-*ras* has been shown to stimulate *Wnt* signalling in colonic cancer through inhibition of *GSK-3beta* (Li *et al.* 2005). *Mapk/Erk* pathway co-operation with *Wnt* signalling pathway could occur at multiple levels, including *via Wnt3a* and *β-catenin/Tcf-4*-dependent gene transcriptional events. *Wnt3a* stimulated G1/S phase cell cycle progression and this stimulation was reduced by an *Erk* pathway inhibitor, indicating that *Wnt3a* promotes proliferation by stimulating the *Erk* pathway (Yun *et al.* 2005; Kim *et al.* 2007).

In intestinal tumours from the K-ras^{Asp12}/*Cre*/$Apc^{Min/+}$ mice, mutated K-*ras* further enhanced expression of *VEGF* compared with that seen in $Apc^{Min/+}$ mouse adenomas. Vascular endothelial growth factor (*VEGF*) is a key regulator of tumour angiogenesis, and angiogenesis is not only restricted to advanced stages of tumour development, but is also observed in benign intestinal adenomas, and *VEGF* can also modulate cellular proliferation, transformation and tumour growth. Mutant K-*ras* up-regulated the expression of *VEGF* in this model and this has been shown previously to occur in a K-*ras/Erk*-dependent and *Wnt*-dependent manner (Jung *et al.*1999; Zhang *et al.* 2001).

The expression of *gastrin*, as a tumour growth factor, is significantly increased in some colorectal cancers compared with the low levels found in normal colonic mucosa. Oncogenic *ras* has been shown to induce *gastrin* gene expression through activation of the *Raf-MEK-ERK* signal transduction pathway (Nakata *et al.* 1998; Koh *et al.* 2000). The *Wnt* signalling pathway moderately stimulates the *gastrin* gene promoter, and Chakladar *et al.* (2005) found a strong (25- to 40-fold) synergistic stimulation of the *gastrin* promoter by the combination of oncogenic *β-catenin* and K-*ras* overexpression. Deletion analysis localized the response element to an area between −140 and −110 bp upstream of the murine *gastrin* promoter. Electrophoretic mobility shift assays detected a complex containing *β-catenin/Tcf*, *AP1*, and *Smad3/4* transcription factors that bound to a DNA element through *AP1* and *Smad* binding sites. *Gastrin* promoter activation could be further enhanced or suppressed by the co-expression of wild type *Smad4* or a dominant negative mutant of *Smad4*, and thus oncogenic *Wnt* and *Ras* signalling pathways can synergistically induce enhanced *gastrin* expression (Chakladar *et al.* 2005). $Apc^{Min/+}$ mice that overexpress one of the alternatively processed forms of *gastrin*, known as glycine-extended *gastrin*, show a significant increase in intestinal adenoma number. Conversely, *gastrin*-deficient $Apc^{Min/+}$ mice showed a marked decrease in intestinal adenoma number and a significantly decreased adenoma proliferation rate (Koh *et al.* 2000). Thus, the real-time qRT-PCR and immunohistochemical data from this study showing that mutated K-*ras* induced enhanced expression of *gastrin* in the adenomas from K-ras^{Asp12}/*Cre*/$Apc^{Min/+}$ mice compared that of Apc^{Min} mice is consistent with these published data.

Cyclo-oxygenase-2 (*Cox2*) has been shown to play a role in the development of intestinal tumours, and *Cox2* levels are elevated in approximately 80–90% of human colorectal carcinomas. Here, we showed increased *Cox2* expression in the large intestine of K-ras^{Asp12}/*Cre* mice and $Apc^{Min/+}$ mice relative to colon from control *Cre* mice, with some immunohistochemical evidence of increased *Cox2* expression in adenomas from K-ras^{Asp12}/*Cre*/$Apc^{Min/+}$ mice. Mutated K-*ras* is associated with increased levels of *Cox2* expression in colorectal carcinomas (Okawa *et al.* 2004). Cyclo-oxygenase 2 (*Cox2*) expression is regulated *via* the *ras* signalling pathway, and induction of mutated *ras* rapidly increases *Cox2* protein levels in intestinal epithelial cells. *Akt* (also known as *protein kinase B*) is an important effector of Ras protein signalling and a critical component of mutant *ras*-mediated transformation. K-*ras*-mediated increase in *cyclo-oxygenase-2* mRNA stability involves activation of the protein kinase B1 (Sheng *et al.* 2001). A *Tcf-4*-binding element (TBE) in the *Cox2* promoter has been identified that specifically binds to Tcf-4 protein in an electrophoretic mobility shift assay. Although *β-catenin* alone did not increase *Cox2* protein to detectable levels in HuH7 cells, co-expression of both mutant *β-catenin* and mutant K-*ras* increased *Cox2* protein expression levels (Araki *et al.* 2003).

We showed some evidence of increased immunohistochemical expression of *Tiam1* (T lymphoma invasion and metastasis 1 gene) in K-ras^{Asp12}/*Cre*/$Apc^{Min/+}$ mouse adenomas. T-cell lymphoma invasion and metastasis 1 (*Tiam1*) has been shown to be an important effector pathway for some of the effects of mutated K-*ras*. $Tiam1^{-/-}$ mice were shown to be resistant to the development of mutant *ras*-induced skin tumours following treatment with the carcinogen 7, 12-dimethylbenzanthracene and promoter 12-O-tetra-decanoylphorbol-13-acetate. Moreover, the few tumours produced in $Tiam1^{-/-}$ mice grew more slowly than those in wild-type mice. T-cell lymphoma invasion and metastasis 1 (*Tiam1*)-deficient primary embryonic fibroblasts were also resistant to ras^{Val12}-induced focus formation.

Hence, *Tiam1* was shown to be a critical regulator of *ras*-induced tumour formation (Malliri *et al.* 2002, 2006; Baines *et al.* 2005). T-cell lymphoma invasion and metastasis 1 (*Tiam1*) is also a *Wnt*-responsive gene expressed in the base of intestinal crypts and up-regulated in Min mouse intestinal adenomas and human colonic adenomas. Moreover, by comparing intestinal tumour development in *Apc* mutant Min mice expressing or lacking *Tiam1*, it was found that *Tiam1* deficiency significantly reduced the formation and growth of intestinal tumours in *vivo* (Malliri *et al.* 2006).

In conclusion, expression of K-ras^{Asp12} alone in the stem cell compartment of the adult intestinal crypt does not significantly initiate adenoma formation, confirming our previous findings for K-ras^{Val12} (Luo *et al.* 2007a) and those of others (Janssen *et al.* 2006; Sansom *et al.* 2006). When crossed on to an $Apc^{Min/+}$ background, the compound mutant K-*ras/Cre/*$Apc^{Min/+}$ mice showed acceleration of intestinal tumour formation, similar to that shown by others crossing mutant K-*ras* and *Apc* mice (Janssen *et al.* 2006; Sansom *et al.* 2006; Calcagno *et al.* 2008; Haigis *et al.* 2008). Although others have shown that the formation of large intestinal adenomas can occur after crossing mutant K-*ras* and *Apc* mice (Calcagno *et al.* 2008; Haigis *et al.* 2008), this study demonstrates the impressive 5.7-fold increase in numbers of adenomas in the large intestine compared with the 1.5-fold increase in the small intestine, more closely mimicking the human situation. However, whereas others have not shown clear evidence of activation of both *Mapk/Akt* and *Wnt/Apc* signalling pathways in the intestinal tumours, the tumour expression studies here showed that mutant K-*ras* increased activation of *Mapk* and *Akt* signalling pathway targets pErk and pAkt, increased expression of the cell cycle entry marker *cyclinD2* and the stem cell markers *Pem*, *Tcl-1* and *Trap*, previously shown to be activated by mutant K-*ras* (Luo *et al.* 2007a,b), as well as increasing the relative gene expression levels of certain *Wnt* pathway targets, such as *VEGF*, *gastrin*, *Cox2* and *Tiam1*. Other *Wnt* pathway target genes such as Peroxisome proliferator-activated receptor delta (*PPARd*), Matrix Metalloproteinase 7 (*MMP7*), *PP1A* and c-*myc* remained unchanged in compound in mutant K-*ras/Cre/*$Apc^{Min/+}$ mouse adenomas compared with $Apc^{Min/+}$ control mouse tumours. Cluster analysis showed a consistent pattern of changes in gene expression in these tumours from K-ras^{Asp12}*/Cre/*$Apc^{Min/+}$ mice, confirming synergistic activity of mutant K-*ras* and mutant *Apc* on their signalling pathways, as previously suggested by others in different experimental systems, but demonstrated here in the large intestinal adenomas forming *in vivo*. Thus, these data showed that intestinal expression of K-ras^{Asp12} accelerates *Apc*-initiated intestinal adenomagenesis *in vivo* with the greater effect on the large intestine and provides an improved mechanistic insight showing that this may be, at least in part, due to synergistic co-operation between the K-*ras/Mapk/Akt* and *Wnt/Apc* pathways resulting in the up-regulation of certain genes.

Acknowledgements

We thank Maggie Green, Clive Lebozer and Xinping Gong (Department of Pathology, University of Cambridge) for technical assistance. This work was supported by grants from CR-UK.

References

Al-Aynati M.M., Radulovich N., Riddell R.H., Tsao M.S. (2004) Epithelial-cadherin and beta-catenin expression changes in pancreatic intraepithelial neoplasia. *Clin. Cancer Res.*, **10**, 1235–1240.

Andreyev H.J., Norman A.R., Cunningham D., Oates J.R., Clarke P.A. (1998) Kirsten ras mutations in patients with colorectal cancer: the multicenter "RASCAL" study. *J. Natl. Cancer Inst.*, **90**, 675–684.

Andreyev H.J., Norman A.R., Cunningham D. *et al.* (2001) Kirsten ras mutation in patients with colorectal cancer: the "RASCAL II" study. *Br. J. Cancer*, **85**, 692–696.

Araki Y., Okamura S., Hussain S.P. *et al.* (2003) Regulation of cyclooxygenase-2 expression by the Wnt and ras pathways. *Cancer Res.* **63**, 728–734.

Arends M.J., Frayling I. (2005). Mismatch repair deficiency in hereditary and sporadic colorectal cancer. In: *The Effective Management of Colorectal Cancer*, 4th edn, pp. 25–40 (eds D. Cunningham, C. Topham, A. Miles), London: Aesculapius Medical Press, Chapter 2.

Arends M.J., McGregor A.H., Toft N.J., Brown E.J., Wyllie A.H. (1993) Susceptibility to apoptosis is differentially regulated by c-myc and mutated Ha-*ras* oncogenes and is associated with endonuclease availability. *Br. J. Cancer*, **68**, 1127–1133.

Arends M.J., McGregor A.H., Wyllie A.H. (1994) Apoptosis is inversely related to necrosis and determines net growth in tumours bearing constitutively expressed myc, ras, and HPV oncogenes. *Am. J. Pathol.*, **144**, 1045–1057.

Baines A.T., Lim K.h., Shields J.M. *et al.* (2005) Use of retrovirus expression of interfering RNA to determine the contribution of activated K-ras and ras effector expression to human tumour cell growth. *Methods Enzymol.*, **407**, 556–574.

Barbacid M. (1987) Ras genes. *Annu. Rev. Biochem.*, **56**, 779–827.

Bos J.L., Fearon E.R., Hamilton S.R. *et al.* (1987) Prevalence of ras gene mutations in human colorectal cancers. *Nature*, **327**, 293–297.

Brooks D.G., James R.M., Patek C.E., Williamson J., Arends M.J. (2001) Mutant K-ras enhances apoptosis in embryonic stem cells in combination with DNA damage and is associated with increased levels of p19 ARF. *Oncogene*, **20**, 2144–2152.

Calcagno S.R., Li S., Colon M. *et al.* (2008) Oncogenic K-ras promotes early carcinogenesis in the mouse proximal colon. *Int. J. Cancer*, **122**, 2462–2470.

Chakladar A., Dubeykovskiy A., Wojtukiewicz L.J., Pratap J., Lei S., Wang T.C. (2005) Synergistic activation of the murine gastrin promoter by oncogenic Ras and beta-catenin involves SMAD recruitment. *Biochem. Biophys. Res. Commun.*, **336**, 190–196.

Chen L.C., Hao C.Y., Chiu Y.S. *et al.* (2004) Alteration of gene expression in normal-appearing colon mucosa of APC^{Min} mice and human cancer patients. *Cancer Res.*, **64**, 3694–3700.

D'Abaco G.M., Whitehead R.H., Burgess A.W. (1996) Synergy between Apc min and an activated ras mutation is sufficient to induce colon carcinomas. *Mol. Cell. Biol.*, **16**, 884–891.

Eisen M.B., Spellman P.T., Brown P.O., Botstein D. (1998) Cluster analysis and display of genome-wide expression patterns. *Proc. Natl. Acad. Sci. U.S.A.*, **95**, 14863–14868.

Ezzell R.M., Chafel M.M., Matsudaira P.T. (1989) Differential localization of *villin* and fimbrin during development of the mouse visceral endoderm and intestinal epithelium. *Development*, **106**, 407–419.

Fearon E.R., Vogelstein B. (1990) A genetic model for colorectal tumourigenesis. *Cell*, **61**, 759–767.

Fearon E.R., Hamilton S.R., Vogelstein B. (1987) Clonal analysis of human colorectal tumours. *Science*, **238**, 193–197.

Guerra C., Mijimolle N., Dhawahir A. *et al.* (2003) Tumor induction by an endogenous K-ras oncogene is highly dependent on cellular context. *Cancer Cell*, **4**, 111–120.

Haigis K.M., Kendall K.R., Wang Y. *et al.* (2008) Differential effects of oncogenic K-Ras and N-Ras on proliferation, differentiation and tumor progression in the colon. *Nat. Genet.*, **40**, 600–608.

Ichii S., Takeda S., Horii A. *et al.* (1993) Detailed analysis of genetic alterations in colorectal tumours from patients with and without familial adenomatous polyposis (FAP). *Oncogene*, **8**, 2399–2405.

Ireland H., Kemp R., Houghton C. *et al.* (2004) Inducible Cre-medated control of gene expression in the murine gastrointestinal tract: effect of loss of β-catenin. *Gastroenterology*, **126**, 1236–1246.

James R.M., Arends M.J., Plowman S. *et al.* (2003) K-ras proto-oncogene exhibits tumour suppressor activity as its absence promotes tumourigenesis in murine teratomas. *Mol. Cancer Res.*, **1**, 820–825.

Janssen K.P., Marjou F.E., Pinto D. *et al.* (2002) Targeted expression of oncogenic K-ras in intestinal epithelium cause spontaneous tumourigenesis in mice. *Gastroenterology*, **123**, 492–504.

Janssen K.P., Abala M., EI Marjou F., Louvard D., Robine S. (2005) Mouse models of K-ras-initiated carcinogenesis. *Biochim. Biophys. Acta*, **1756**, 145–154.

Janssen K.P., Alberici P., Fsihi H. *et al.* (2006) APC and oncogenic KRAS are synergistic in enhancing Wnt signaling in intestinal tumor formation and progression. *Gastroenterology*, **131**, 1096–1109.

Johnson L., Mercer K., Greenbaum D. *et al.* (2001) Somatic activation of the K-ras oncogene causes early onset lung cancer in mice. *Nature*, **410**, 1111–1116.

Johnson N.A., Hamoudi R.A., Ichimura K. *et al.* (2006) Application of array CGH on archival formalin-fixed paraffin-embedded tissues including small numbers of microdissected cells. *Lab. Invest.*, **86**, 968–978.

Jung Y.D., Nakano K., Liu W., Gallick G., Ellis L. (1999) Extracellular signal-regulated kinase activation is required for up-regulation of vascular endothelial growth factor by serum starvation in human colon carcinoma cells. *Cancer Res.*, **59**, 4804–4807.

Kim S.H., Roth K.A., Moser A.R., Gordon J.I. (1993) Transgenic mouse models that explore the multistep hypothesis of intestinal neoplasia. *J. Cell Biol.*, **123**, 877–893.

Kim S.E., Lee W.J., Choi K.Y. (2007) The PI3 kinase-Akt pathway mediates Wnt3a-induced proliferation. *Cell. Signal.*, **19**, 511–518.

Koh T., Bulitta C., Fleming J., Dockray G., Varro A., Wang T. (2000) Gastrin is a target of the ß-catenin/TCF-4 growth-signaling pathway in a model of intestinal polyposis. *J Clin. Invest.*, **106**, 533–539.

Levy D.B., Smith K.J., Beazer-Barclay Y., Hamilton S.R., Vogelstein B., Kinzler K.W. (1994) Inactivation of both APC alleles in human and mouse tumours. *Cancer Res.*, **54**, 5953–5958.

Li J., Mizukami Y., Zhang X., Jo W.S., Chung D.C. (2005) Oncogenic K-*ras* stimulates Wnt signaling in colon cancer through inhibition of GSK-3 beta. *Gastroenterology*, **128**, 1907–1918.

Luo F., Brooks D.G., Ye H. *et al.* (2007a) Conditional expression of mutated K-*ras* accelerates intestinal tumourigenesis in Msh2-deficient mice. *Oncogene*, **26**, 4415–4427.

Luo F., Hamoudi R., Brooks D.G., Patek C.E., Arends M.J. (2007b) Stem cell gene expression changes induced specifically by mutated K-*ras*. *Gene Expr.*, **14**, 101–115.

Maher J., Baker D.A., Manning M., Dibb N.J., Roberts I.A.G. (1995) Evidence for cell-specific differences in transformation by N-, H- and K-ras. *Oncogene*, **11**, 1639–1647.

Malliri A., van der kammen R.A., Clark K., van der Valk M., Michiels F., Collard J. (2002) Mice deficient in the Rac activator Tiam1 are resistant to Ras-induced skin tumours. *Nature*, **417**, 867–871.

Malliri A., Rygiel T.P., van der Kammen R.A. *et al.* (2006) The rac activator Tiam1 is a Wnt-responsive gene that modifies intestinal tumor development. *J. Biol. Chem.*, **281**, 543–548.

Malumbres M., Barbacid M. (2003) RAS oncogenes: the first 30 years. *Nat. Rev. Cancer*, **3**, 459–465.

Morris R.G., Curtis L.J., Romanowski P. *et al.* (1996) Ki-ras mutations in adenomas: a characteristic of cancer-bearing colorectal mucosa. *J. Pathol.*, **180**, 357–363.

Nakata H., Wang S.-L., Chung D.C., Westwick J.K., Tillotson L.G. (1998) Oncogenic *ras* induces gastrin gene expression in colon cancer. *Gastroenterology*, **115**, 1144–1153.

Ohnishi T., Tomita N., Monden T. *et al.* (1997) A detailed analysis of the role of K-*ras* gene mutation in the progression of colorectal adenoma. *Br. J. Cancer*, **75**, 341–347.

Okawa T., Yoshinaga K., Uetake H. *et al.* (2004) Cyclooxygenase-2 overexpression is related to polypoid growth and K-ras gene mutation in T1 colorectal carcinomas. *Dis. Colon Rectum*, **47**, 1915–1921.

Otori K., Oda Y., Sugiyama K. *et al.* (1997) High frequency of K-ras mutations in human colorectal hyperplastic polyps. *Gut*, **40**, 660–663.

Powell S., Zilz N., Beazer-Barclay Y. *et al.* (1992) *APC* mutations occur early during colorectal tumourigenesis. *Nature*, **359**, 235–237.

Robine S., Huet C., Moll R. *et al.* (1985) Can villin be used to identify malignant and undifferentiated normal digestive epithelial cells? *Proc. Natl. Acad. Sci. U.S.A.*, **24**, 8488–8492.

Rustgi A.K. (1994) Hereditary gastrointestinal polyposis and nonpolyposis syndromes. *N. Engl. J. Med.*, **331**, 1694–1702.

Sansom O.J., Meniel V., Wilkins J.A. *et al.* (2006) Loss of Apc allows phenotypic manifestation of the transforming properties of an endogenous K-ras oncogene in vivo. *Proc. Natl. Acad. Sci. U.S.A.*, **103**, 14122–14127.

Sheng H., Shao J., Dubois R.N. (2001) K-Ras-mediated increase in cyclooxygenase 2 mRNA stability involves activation of the protein kinase B1. *Cancer Res.*, **61**, 2670–2675.

Shivapurkar N., Huang L., Ruggeri B. *et al.* (1997) K-ras and p53 mutations in aberrant crypt foci and colonic tumours from colon cancer patients. *Cancer Lett.*, **115**, 39–46.

Sjöblom T., Jones S., Wood L.D. *et al.* (2006) The consensus coding sequences of human breast and colorectal cancers. *Science*, **314**, 268–274.

Spandidos D.A., Wilkie N.M. (1984) Malignant transformation of early passage rodent cells by a single mutated human oncogene. *Nature*, **310**, 469–475.

Su L.K., Kinzler K.W., Vogelstein B. *et al.* (1992) Multiple intestinal neoplasia caused by a mutation in the murine homolog of the APC gene. *Science*, **256**, 668–670.

Takayama T., Ohi M., Hayashi T. *et al.* (2001) Analysis of K-ras, APC, and beta-catenin in aberrant crypt foci in sporadic adenoma, cancer, and familial adenomatous polyposis. *Gastroenterology*, **121**, 599–611.

Tuveson D.A., Shaw A.T., Willis N.A. *et al.* (2004) Endogenous oncogenic K-ras(G12D) stimulates proliferation and widespread neoplastic and developmental defects. *Cancer Cell*, **5**, 375–387.

Wood L.D., Parsons D.W., Jones S. *et al.* (2007) The genomic landscapes of human breast and colorectal cancers. *Science*, **318**, 1108–1113.

Yun M.S., Kim S.E., Jeon S.H., Lee J.S., Choi K.Y. (2005) Both ERK and Wnt/beta-catenin pathways are involved in Wnt3a-induced proliferation. *J. Cell Sci.*, **118**, 313–322.

Zhang X., Gaspard J.P., Chung D.C. (2001) Regulation of vascular endothelial growth factor by the Wnt and K-ras pathways in colonic neoplasia. *Cancer Res.*, **61**, 6050–6054.